

Small-Angle Cross Sections for the Scattering of Protons by Tritons*

MALCOLM E. ENNIS AND ARTHUR HEMMENDINGER

University of California, Los Alamos Scientific Laboratory, Los Alamos, New Mexico

(Received April 5, 1954)

The proton-triton differential scattering cross section has been measured for center-of-mass angles between 20° and 150° and proton energies in the range 1 to 2.55 Mev. Probable errors vary between 3 and 5 percent.

INTRODUCTION

AN analysis by McIntosh, Gluckstern, and Sack¹ of two sets of proton-triton scattering data^{2,3} presents two possible sets of phase shifts, one of which implies the existence of a singlet P resonance in He^4 , the other of which is nonresonant. To date no differential cross sections have been reported for laboratory angles less than 45 degrees, and it is in this range that the calculated differential cross sections are most sensitive to the choice of phase shifts. These measurements were undertaken with the hope that, even if they do not lead to unique values of phase shifts, they might help answer the question of the existence of a singlet P resonance in He^4 .

In both earlier experiments small volume scattering chambers were used, similar to that first described by Taschek⁴; these chambers cannot be used at small angles, and they are difficult to use for tritium because with such a small volume-to-surface ratio rapid changes in isotopic composition occur. The present experiment was undertaken with a large chamber, 14 inches in diameter and 4 inches high, a complete description of which is given by Sherr *et al.*⁵

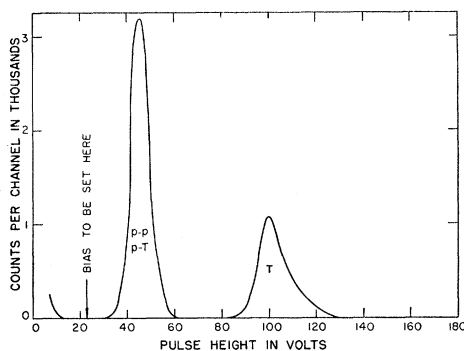


FIG. 1. Pulse-height distribution for the monitor counter showing the bias setting for the integral discriminator.

* Work done under the auspices of the U. S. Atomic Energy Commission.

¹ McIntosh, Gluckstern, and Sack, *Phys. Rev.* **88**, 752 (1952).

² Hemmendinger, Jarvis, and Taschek, *Phys. Rev.* **76**, 1137 (1949).

³ Claassen, Brown, Freier, and Stratton, *Phys. Rev.* **82**, 589 (1951).

⁴ R. F. Taschek, *Rev. Sci. Instr.* **19**, 591 (1948).

⁵ Sherr, Blair, Kratz, Bailey, and Taschek, *Phys. Rev.* **72**, 662 (1947).

APPARATUS

The proton beam was provided by the Los Alamos 2.5-Mev electrostatic accelerator A , the same one used in the earlier scattering measurements.²

The current collector described by Sherr⁵ was modified so that it remained close to ground potential and was isolated from electron currents by a cylindrical barrier electrode at a potential of -250 volts located just in front of the collector.

The target gas was confined by an entrance foil of 0.16-mil aluminum, an exit foil of 0.05-mil nickel, and two counter foils each of 0.05-mil nickel. The pressure of this gas was measured, through a liquid nitrogen trap, by a 0-20-mm Wallace and Tiernan differential pressure gauge used as a null indicator, with an oil manometer to indicate pressure on the static side of the gauge.

The dimensions of the movable-counter collimator were, in the usual notation,⁶ $A=1.807 \times 10^{-2}$ cm², $2b=0.2111$ cm, $h=6.982$ cm, $R=12.893$ cm, from which we find $G=4.242 \times 10^{-5}$ cm.

The counter fillings were 25 or 50 cm pressure of argon plus 7 percent of carbon dioxide. Counter anodes were 5-mil wires, at a voltage of 1150 or 1450. The energy resolution of the counters, about 15 percent with a new gas filling, deteriorated slowly, so that the counters needed refilling every day.

Tritium, stored in a uranium furnace, was readily pumped into or out of the chamber; each pumping cycle separated hydrogen isotopes from the contaminants that grew slowly in the chamber.

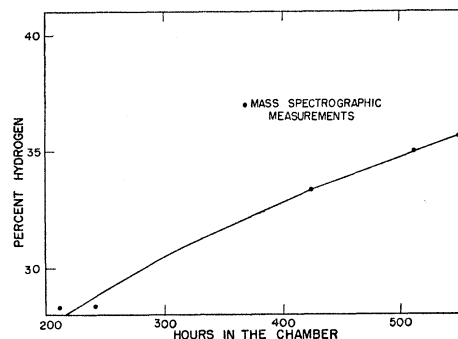


FIG. 2. The growth of hydrogen in the chamber, used for interpolation between mass spectroscopic measurements.

⁶ Breit, Thaxton, and Eisenbud, *Phys. Rev.* **55**, 1018 (1939).

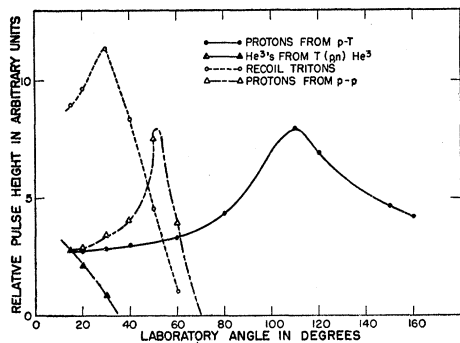


FIG. 3. A representative set of curves, for 50-cm counter pressure (argon) and 2.548-Mev incident proton energy, showing the pulse height due to various scattered and reaction particles as a function of angle.

Electronic circuits were the same as those described by Sherr, with the substitution of a new 18-channel pulse-height analyzer⁷ for the older 10-channel analyzer.

EXPERIMENTAL PROCEDURE

The yield in counts per microcoulomb of beam current integral at the angle ϑ as a function of the differential scattering cross section $\sigma(\vartheta)$ is

$$Y = Nn\sigma(\vartheta)G \csc\vartheta, \quad (1)$$

where $N = 6.250 \times 10^{12}$ protons/microcoulomb, n = number of scattering particles per cubic centimeter, and G = the geometry factor ($= 4.242 \times 10^{-5}$ cm).

The thickness of the entrance foil was determined by measuring the $T^3(p,n)$ threshold with a few millimeters pressure of tritium in the chamber, and later with no foil and a zirconium-tritium target, in each case using a long counter to detect neutrons.

The monitor counter at 14 degrees, with the bias set carefully at the minimum shown in Fig. 1 between background and the smallest peak in pulse height, was used instead of a current integrator and was calibrated at a known temperature and pressure of chamber gas in terms of the charge collected in the Faraday cage as measured by a ballistic galvanometer. Frequent calibration was required because the heavy contaminant in the chamber gas grew at the rate of 0.06 percent per hour.

Whenever the tritium was pumped into the uranium trap a background run was made on the residual gas to correct tritium scattering data, especially at small angles. After each two days of running time a mass spectrometric determination of tritium concentration was made. Hydrogen concentration at intermediate times was evaluated from the curve of Fig. 2. The liquid nitrogen trap connected to the chamber was kept full whenever there was a beam through the chamber to minimize the rate of deposition of carbon films on the foils.

⁷ C. W. Johnstone, *Nucleonics* **11**, 36 (1953).

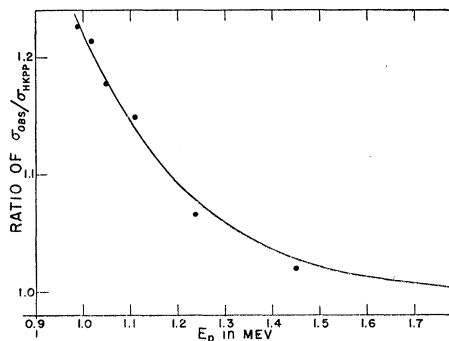


FIG. 4. Measurements of the proton-proton scattering cross section, at various angles, plotted as the ratio to the HKPP measurements as a function of energy. The smooth curve was used to show the ratio of observed Faraday cage current to the actual current that would be observed in the absence of gas scattering.

ANALYSIS OF DATA

The various scattered and recoil groups traversing the counter, including at some angles and energies the recoils from the reaction $T^3(p,n)He^3$, produced such a multiplicity of peaks that any one could be identified only after calculation of particle energetics and energy losses in target gas, foil, counter, as shown in Fig. 3. When the peak due to $p-p$ protons overlapped that due to $p-T$ protons at small angles, it was necessary to subtract the calculated $p-p$ yield from the total, using the mass spectrometric hydrogen concentration and the known values for the $p-p$ cross section.⁸ Equation (1) for the $p-T$ cross section then becomes

$$\sigma = \frac{Y \sin\theta}{n_1 N G P_T} - \frac{P_H}{P_T} \sigma_1, \quad (2)$$

where n_1 is the number of atoms in a diatomic gas per cubic centimeter at 1 cm of mercury pressure, P_T is the partial pressure of tritium, P_H is the partial pressure of hydrogen, and σ_1 is the $p-p$ scattering cross section. Except for the two points at 120 degrees laboratory angle all of the large angle data are calculated from yields of recoil tritons at small angles. At the higher energies, recoil-triton and scattered-proton data join neatly.

Often a group was superposed on the "tail" of another group—a tail on the low-energy side produced by small-angle secondary scattering in gas or slit edges—in which case the pulse distributions were plotted, tails were drawn by extrapolation, and suitable subtractions were made.

Small counter backgrounds due to recoils from $T(p,n)$ neutrons and possibly from gamma pileup were measured by moving a magnetically operated shutter into the beam entering the counter; these corrections were never greater than a few percent.

At the lower beam energies an appreciable fraction

⁸ Herb, Kerst, Parkinson, and Plain, *Phys. Rev.* **55**, 998 (1939); referred to later as HKPP.

of the incident proton beam was scattered into angles greater than that subtended by the Faraday cage. Corrections to the current integral, determined by the yield of protons scattered from the hydrogen diluent in the tritium, became appreciable below 1.3 Mev and rose to 20 percent at 1.0 Mev. Figure 4 shows a smooth curve for scattering of protons out of the incident beam determined by experimental points, from which corrections were taken.

An approximate calculation of the loss of once-scattered particles from the beam entering the counter due to secondary gas scattering shows that it is largely self compensating in that there will be as many particles scattered into the beam as there are lost to the beam. The correction due to the use of a counter subtending a finite solid angle to measure an angular

distribution that has a large second derivative proves to be less than 0.5 percent and was neglected.

The correction due to heavy contaminants, determined by "pumping" out the tritium and scattering from the residual chamber gas, was about 1 percent.

RESULTS

In Table I are shown the averages of all measurements weighted inversely as their probable errors. The number of runs per point is between 1 and 12, with most of the data falling near the middle of this range. A comparison of the three sets of p -T scattering data at energies selected is shown in Fig. 5.

The probable error in the mean energy of the incident protons corrected for energy loss in the entrance foil and target gas is ± 5 kev.

TABLE I. The p -T cross sections in both laboratory and center-of-mass systems.^a

Lab. angle θ	C.m. angle Ω	$E_p=0.990$ Mev		$E_p=1.019$ Mev		$E_p=1.049$ Mev		$E_p=1.108$ Mev		$E_p=1.236$ Mev		$E_p=1.450$ Mev	
		σ_θ	σ_Ω										
15	20	4.043	2.314	3.997	2.287	3.751	2.147	3.364	1.925	2.733	1.564	2.010	1.150
20	26.6	1.300	0.756	1.277	0.742	1.208	0.702	1.016	0.590	0.905	0.526	0.723	0.420
25	33.1	0.627	0.371	0.617	0.366	0.562	0.333	0.489	0.290			0.415	0.246
30	39.6	0.394	0.239	0.378	0.229	0.332	0.201	0.315	0.191	0.291	0.176	0.316	0.192
35	46.0	0.303	0.189	0.305	0.190	0.278	0.173	0.234	0.146			0.263	0.164
40	52.4	0.265	0.171	0.253	0.163	0.239	0.154	0.215	0.138	0.213	0.137	0.236	0.152
45	58.7	0.260	0.173	0.240	0.160	0.215	0.143	0.189	0.126	0.181	0.121	0.217	0.145
50	64.8	0.231	0.160	0.224	0.155	0.193	0.134	0.181	0.125	0.180	0.125	0.199	0.138
55	70.9												
60	76.8			0.205	0.155							0.165	0.125
62.8	80												
71.6	90											0.156	0.133
80.8	100									0.167	0.158	0.152	0.144
90.5	110											0.150	0.160
100.9	120	0.163	0.198	0.161	0.196	0.155	0.188	0.152	0.185	0.158	0.185	0.157	0.191
112.0	130	0.160	0.223	0.151	0.210	0.150	0.209	0.151	0.210			0.157	0.219
120	136.8									0.148	0.227		
123.9	140	0.146	0.234	0.148	0.239	0.144	0.231	0.141	0.226	0.152	0.243	0.157	0.251
136.8	150	0.150	0.274	0.140	0.256	0.137	0.250	0.141	0.258	0.148	0.270	0.157	0.287
Lab. angle θ	C.m. angle Ω	$E_p=1.678$ Mev		$E_p=1.900$ Mev		$E_p=2.117$ Mev		$E_p=2.335$ Mev		$E_p=2.548$ Mev			
		σ_θ	σ_Ω										
15	20	1.458	0.834	1.207	0.691	1.062	0.608	0.958	0.548	1.020	0.584		
20	26.6	0.606	0.352	0.565	0.328	0.591	0.343	0.622	0.362	0.697	0.405		
25	33.1	0.389	0.230	0.417	0.247	0.477	0.283	0.528	0.313	0.578	0.342		
30	39.6	0.353	0.214	0.366	0.222	0.418	0.253	0.447	0.271	0.495	0.300		
35	46.0	0.308	0.192	0.333	0.207	0.368	0.229	0.369	0.230	0.421	0.262		
40	52.4	0.275	0.177	0.280	0.180	0.310	0.199	0.355	0.228	0.358	0.230		
45	58.7	0.237	0.158	0.240	0.160	0.265	0.176			0.320	0.213		
50	64.8	0.211	0.146	0.218	0.151			0.242	0.168	0.257	0.178		
55	70.9					0.190	0.137						
60	76.8	0.171	0.129	0.157	0.119	0.172	0.130	0.160	0.121	0.186	0.141		
62.8	80			0.155	0.121			0.149	0.116	0.161	0.126		
71.6	90	0.127	0.108	0.132	0.113	0.128	0.109			0.119	0.102		
80.8	100	0.139	0.132	0.130	0.123	0.119	0.113	0.104	0.099	0.101	0.096		
90.5	110	0.138	0.147	0.129	0.138	0.118	0.126	0.109	0.116	0.098	0.105		
100.9	120	0.147	0.179	0.136	0.165	0.132	0.160	0.113	0.137	0.106	0.129		
112.0	130	0.154	0.215	0.145	0.202	0.134	0.187	0.129	0.180	0.112	0.156		
120	136.8	0.133	0.204										
123.9	140	0.152	0.243	0.150	0.240	0.143	0.229	0.131	0.210	0.121	0.194		
136.8	150	0.147	0.268	0.147	0.268	0.144	0.263	0.134	0.245	0.125	0.228		

^a The probable errors in these cross sections are as follows:

$E_p=0.990$ to 1.108 Mev—5 percent.

$E_p=1.236$ and 1.450 Mev—3 percent.

$E_p=1.678$ to 2.548 Mev—4 percent above the horizontal line and 3 percent below.

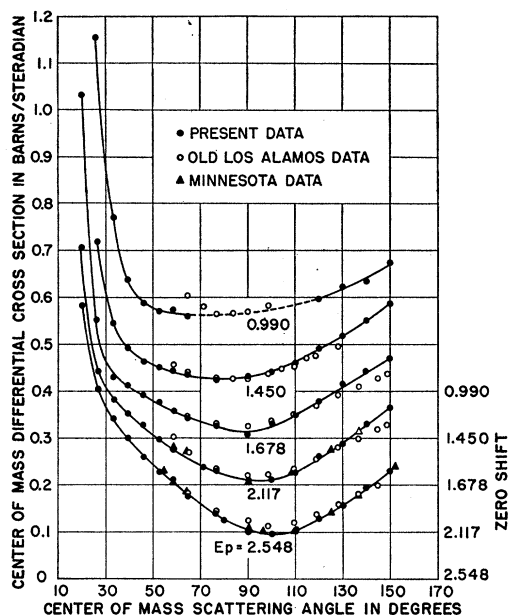


FIG. 5. The p -T cross section as a function of angle (c.m. system) for five energies, including all of the earlier measurements at the energies selected.

Estimates of probable errors in cross sections and their sources are as follows:

- Y , 2.5 percent due to statistics;
- P_T , 0.5 percent due to pressure measurement,
0.7 percent due to isotopic composition;
- P_H , 0.5 percent due to pressure measurement,
2.0 percent due to isotopic composition;
- G ,* 0.5 percent due to distance measurements.

The errors in cross section approximate 3 percent, except where the subtraction indicated in Eq. (2) must be performed, where they are 5 percent. At the lowest energies there is an additional error, possibly as great as 3 percent, due to the correction of the current integral for scattering out of the beam.

* *Note added in proof.*—Shortly before receiving the galley proofs, one of the authors (A. H.) removed the entrance foil of the movable counter and found that about 1.5 percent of the hole A was covered with wax. The authors will send to anyone requesting it a table of cross sections calculated using a corrected geometry factor.

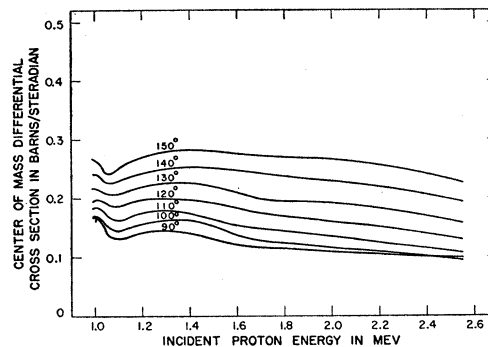


FIG. 6. The p -T cross section as a function of energy (c.m. system) for large angles, showing the minimum near 1-Mev proton energy.

Comparison of the present work with earlier measurements² confirms the observation of a minimum in the center-of-mass cross section as a function of energy near the $T(p,n)$ threshold, as predicted in a theory of Wigner.⁹ The general trend, more pronounced for large angles, is shown in Fig. 6. This particular feature in the earlier work was somewhat in doubt because of the energy and angle straggling in the Faraday cage foil.

The 20-degree center-of-mass differential cross section calculated from the eight phase-shift "fits" given by McIntosh *et al.* for the 2.5-Mev Minnesota data give two good fits for the small angles, of which one,

$${}^1K_0=64^\circ, {}^3K_0=64^\circ, {}^1K_1=-60^\circ, {}^3K_1=3^\circ, \quad (A)$$

is resonant (large singlet p phase shift) and the other,

$${}^1K_0=64^\circ, {}^3K_0=64^\circ, {}^1K_1=46^\circ, {}^3K_1=-16^\circ, \quad (B)$$

is not. The resonant fit is slightly better than the non-resonant, but each fit might be improved by including a small amount of d wave. Actually the existence of an appreciable d -wave component appears plausible in the light of recent angular distribution measurements for $T^3(p,n)$ by Willard and collaborators,¹⁰ and it is demanded by the angular distributions for $T^3(p,\gamma)$ measured by Perry and Bame.¹¹

⁹ E. P. Wigner, Phys. Rev. **73**, 1002 (1948).

¹⁰ Willard, Bair, and Kington, Phys. Rev. **90**, 865 (1953).

¹¹ J. E. Perry and S. J. Bame, Phys. Rev. **90**, 380 (1953).